BELGICA-7904: A NEW CARBONACEOUS CHONDRITE FROM ANTARCTICA; MINOR-ELEMENT CHEMISTRY OF OLIVINE

C. SKIRIUS, I. M. STEELE and J. V. SMITH

Department of the Geophysical Sciences, The University of Chicago, Chicago, Illinois 60637, U.S.A.

Abstract: Belgica-7904 is an unusual C2 meteorite which lacks pyroxene. It contains two groups of clasts, and three types of olivine distinguished by red, blue or no cathodoluminescence. Seven clasts in the first group are characterized by red forsterite (Fo_{99-98}) in a cryptocrystalline greenish-brown matrix. The red forsterite is subhedral, equigranular, and contains numerous brown and Ni-Fe inclusions. One of these clasts contains inclusion-free blue forsterite grains with red margins. These seven clasts are encircled by an opaque rim. Two clasts of the second group have no opaque rim, and consist of blocky to euhedral Fe-rich olivine (first Fo_{83-67}; second Fo_{56-41}) which lack luminescence. The second of these clasts contains a small grain of blue forsterite rimmed by Fe-rich olivine. The forsterites show unusually high levels of the refractory elements Al, Ca and Ti with positive intercorrelations; blue ones have higher concentrations than most red ones. Manganese, Cr and Fe show strong positive correlations with lower concentrations in the blue olivines; they are negatively correlated with Al, Ca and Ti. The Fe-rich olivines of the second clast group have lower levels of Ca, Ti and Al. It is proposed tentatively that the inclusion-free blue forsterites may be relic grains formed by condensation from a vapor rich in refractory elements, and that the inclusion-bearing red forsterite and the non-luminescent Fe-rich olivines formed from separate liquids. Pyroxene is absent from both the clasts and separate mineral grains. The minor-element chemistry of the forsterites in B-7904 is different from that for Allende (CV3), and is similar to that for one group of forsterites in Murchison (C2). It is certain that the olivines in B-7904 require a complex history probably involving initial condensation from a refractory-rich vapor, partial melting and reaction with other materials, and crystallization from more than one type of melt. The minor-element chemistry and textures of olivines in the chondritic meteorites should prove important in deciphering the details of these processes, as well as in classification between and within the groups of carbonaceous chondrites.

1. Introduction

The relationships between stratospheric dust collected by high-flying aircraft (BROWNLEE *et al.*, 1977), deep-sea particles which have partly or completely melted during passage through the atmosphere (BROWNLEE, 1981; BROWNLEE *et al.*, 1984), and carbonaceous chondrites are crucial to discussions about comets and asteroids. Particularly valuable are the textural relations and minor-element signatures of Mg-rich olivines which occur in all the above materials and are sufficiently refractory to

survive transient heating. In particular, there are distinct differences between forsterites from the Murchison (C2), Allende (CV3) and Orgueil (C1) carbonaceous meteorites (STEELE *et al.*, 1985a), and the relic olivines in deep-sea particles can be matched only with those in Murchison and Belgica-7904 (B-7904) carbonaceous meteorites (STEELE *et al.*, 1985b). We have now embarked on a systematic study of Mg-rich olivines in meteorites to provide a comprehensive data base for intercomparison: in particular, we expect to find variations among the C2 meteorites, and we hope to obtain useful clues to the origin of relic olivines in ordinary chondrites (RAMBALDI, 1981) and enstatite chondrites (RAMBALDI *et al.*, 1983). In addition, we are using cathodoluminescence and minor-element analyses to test the dispute about the relationships between isolated olivine grains and those in chondrules of C2 meteorites (FUCHS *et al.*, 1973; OLSEN and GROSSMAN, 1978; MCSWEEN, 1977b; RICHARDSON and MCSWEEN, 1978). On the one hand isolated olivine grains are considered to be direct condensates while the opposing view maintains that they represent grains of preexisting chondrules which have been fractured. We believe that the minor element signature of olivine should reflect the mechanism of formation of the original olivine or the reservoir from which the olivine formed.

As part of this comprehensive study, we present a detailed description of the B-7904 meteorite which was collected by the Japanese Antarctic Research Expedition of 1979. This was originally described as a C2(CM) chondrite with amoeboid olivine and small, Ca,Al-rich inclusions in an abundant dark phyllosilicate matrix (NATIONAL INSTITUTE OF POLAR RESEARCH, 1982). We presented a preliminary description (STEELE *et al.*, 1984) suggesting that this meteorite may be an unusual C2 meteorite, in that pyroxene is absent from the chondrules, there are no CAI's, the inclusion/matrix ratio is low, and the glass is devitrified. These unusual features, as well as our interest in olivine chemistry, have prompted us to examine in detail the texture and minor element signature of the B-7904 olivines. In the following, it should be kept in mind that the thin section available is of small area and is not necessarily representative of the whole 1.234 kg meteorite.

2. Petrographic Description

The sample available for study is a polished thin section (B-7904,92-3) of ~ 19 mm^2 area (Fig. 1.). Petrographic examination showed eight larger clasts (labeled 1–8) ranging up to 1 mm in diameter, each composed of polygranular olivine with interstitial glass (Figs. 2 and 3). In addition, numerous single olivine grains and distinctly smaller polygranular clasts (*e.g.* clast #9; Fig. 3) are dispersed within the opaque to brown phyllosilicate matrix. Figure 1a presents an overall view of the thin section with most large clasts identified while Fig. 1b illustrates features found in the general matrix. The term clast is used rather than chondrule to avoid any possible genetic implication.

2.1. Clasts

The eight larger clasts are described in detail in the Appendix, and a photomicrograph of each is given in Figs. 2 and 3. They can be divided into two groups (1–6 and

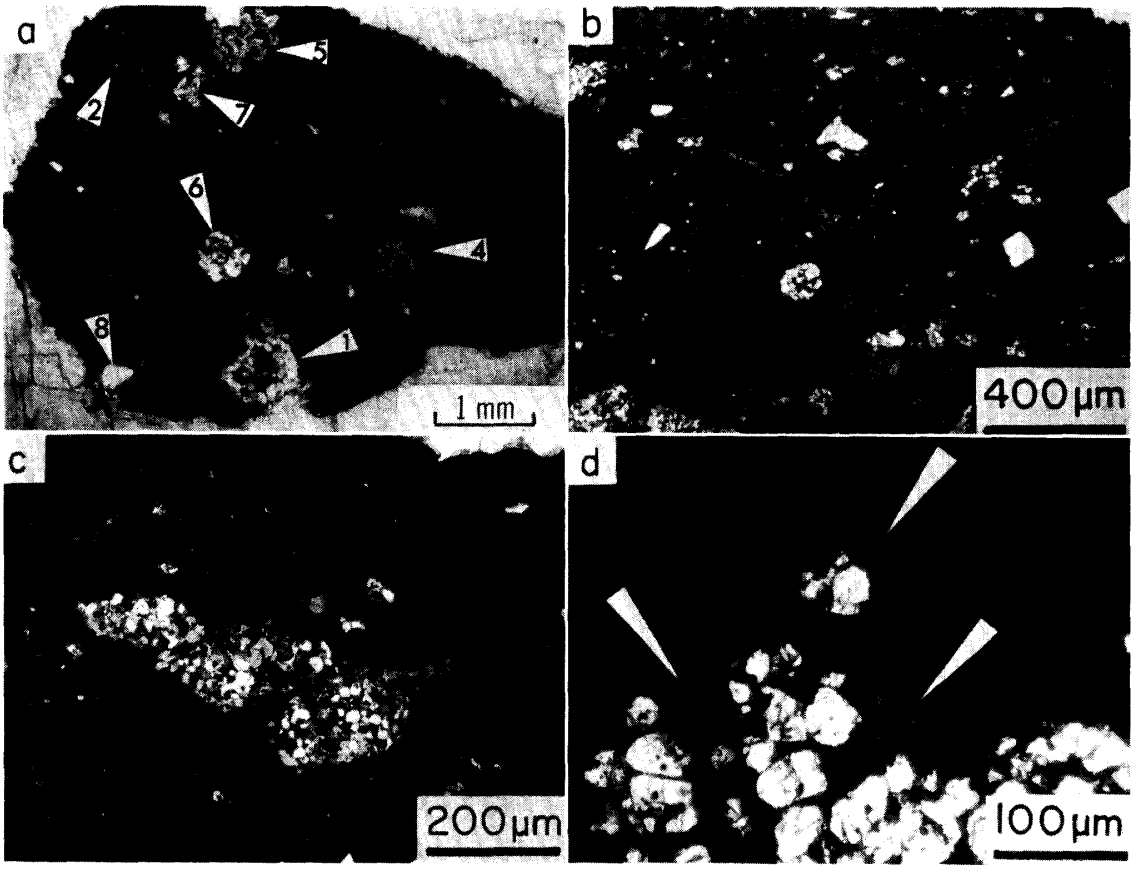

Fig. 1. Transmitted-light photomicrographs of B-7904.

a. Entire thin section, except for clast #3 which is off the right edge.

b. Enlarged area above clast #8, but rotated 90° anticlockwise. Mineral and polygranular clasts 100 µm or less occur in an almost opaque phyllosilicate matrix.

c. Enlarged area to the left of clast #6, but rotated 70° anticlockwise. A small granular clast is surrounded by an ~50 µm thick zone of opaque matrix which contains no inclusions.

d. Enlargement of clast #4 illustrating three areas (arrows) which are brown and isotropic, but with similar morphology to the adjacent olivine.

7–8) based on major and minor element chemistry of olivine, olivine texture, and clast-matrix textural relations.

Clasts #1–6 are composed of equigranular subhedral to rounded olivine in a matrix of greenish-brown cryptocrystalline material interpreted as devitrified glass. They could be classed as Type I chondrules (McSween, 1977a). For these six clasts, the ratio of green-brown matrix/olivine ranges from 4: 1 for clast #1 to 1: 2 for clast #4. The outlines of these clasts range from amoeboid (#2) to subround (#1) with some having angular protrusions (*e.g.* #4). Clast #1 has a distinctly concentric distribution of textures. Each of these 6 clasts is surrounded by a matrix shell 10–100 mm thick which is distinct from the general meteorite matrix in that it contains only rare inclusions and thus appears opaque (Fig. 1c). This shell tends to give a rounder outline to each clast by filling recesses. The inner boundary of this shell against the clast is always sharp while the outer boundary against the general matrix is gradual. Clasts #7–8 do not have this shell.

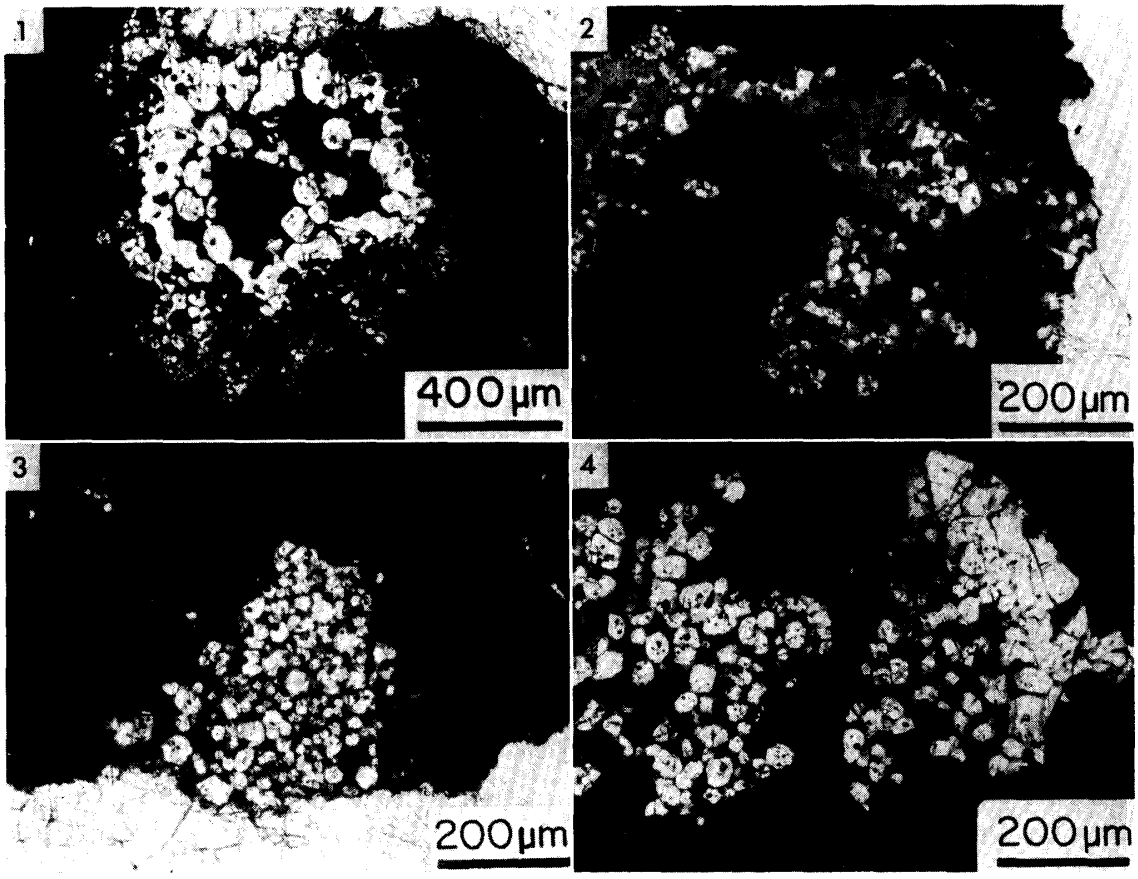

Fig. 2. Transmitted-light photomicrographs of clasts #1–4 from Fig. 1.

The olivine grains in clasts #1–6 have numerous ~10 mm greenish-brown inclusions similar in color to that of the glassy matrix within each clast; micrometer inclusions of Ni-bearing iron and Fe-sulfide are less common. While the matrix of each clast is rather uniformly greenish-brown, some areas similar in size to the olivine grains are isotropic rather than cryptocrystalline and appear as if they are pseudomorphs after olivine. These features can be especially well seen in clasts #4 (left half), #6 and #3. Most of the isotropic grains occur at the periphery. Figure 1d shows a portion of clast #4 with these areas noted. Other features, especially evident in clast #6, are ragged olivine grains into which the greenish-brown matrix appears to penetrate as if reacting with the olivine.

The two clasts (7, 8) forming the second group contain distinctly larger and blocky to euhedral olivine grains relative to clasts #1–6. The olivine contains only rare inclusions and the green-brown matrix forms less than 10% of the area. These two clasts also contain chromite, tiny phosphates, Fe-Ni sulfide, and Fe-Ni. Based on texture and mineralogy, they are similar to Type II chondrules (MCSWEEN, 1977a).

Cathodoluminescence photography (next section) revealed three types of olivine with red, blue or no optical luminescence. All the olivines in clasts #1–6 have red luminescence except for blue grains in a band at the upper-right of the right-hand part of clast #4 (Fig. 2). This band is texturally quite different from the rest of the clast. Blue grains at the edge of the band have red margins, and the textural features

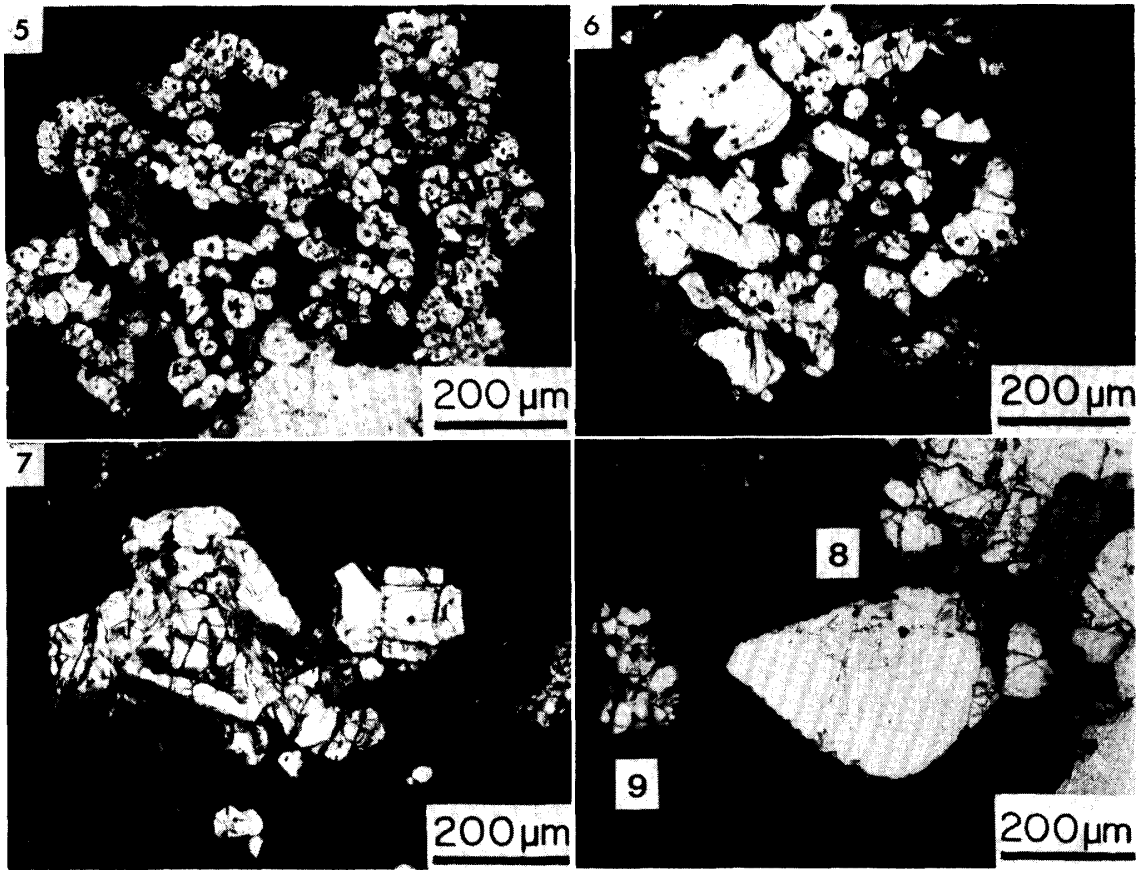

Fig. 3. Transmitted-light photomicrographs of clasts #5–9 from Fig. 1.

suggest that the red olivine was added in some way to preexisting blue grains. All the olivines in clast #8 lack luminescence, as do the larger grains in clast #7. Because the inner part of a small grain of clast #7 has blue luminescence, and the outer part lacks luminescence, it again appears that the blue grains were earlier than other olivines.

2.2. Matrix

The general matrix shows a uniform dark-brown translucent color with numerous tiny polycrystalline and mineral clasts (Figs. 1b, 1c). Most of the mineral clasts are olivine, and a few grains of whitlockite and chromite occur. Prolonged search did not reveal grains of Mg-pyroxene. There is a subtle banding of clasts and mineral grains from the upper left to lower right of Fig. 1a which is more evident in the microscope than in the photomicrograph. The larger clasts do not show a preferred elongation, but some of the smaller clasts do. Examination of larger slices of the meteorite is desirable to follow up this hint of a sedimentary texture.

3. Experimental Techniques

Because olivine is the major phase in both the polygranular clasts and mineral grains, the electron microprobe was set up for long counting times to give high precision for minor elements.

Table 1. Selected analyses of olivine.

Clast	1	2	3	4	4	4	4	4	5	6	7	7
Type	R	R	R	Bc	Rr	Bc	Rr	B	R	R	B	B
SiO_2	42.8	43.6	43.1	42.2	42.3	42.0	41.9	42.6	42.5	41.9	41.9	42.3
TiO_2	0.038	0.015	0.042	0.059	0.058	0.057	0.042	0.061	0.050	0.052	0.073	0.056
Al_2O_3	0.041	0.081	0.165	0.320	0.237	0.236	0.176	0.275	0.138	0.152	0.214	0.216
Cr_2O_3	0.416	0.498	0.304	0.127	0.442	0.163	0.398	0.183	0.275	0.350	0.225	0.193
FeO	0.897	0.942	0.705	0.965	0.961	0.824	1.040	0.787	0.964	0.946	0.841	0.767
MnO	0.077	0.167	0.065	0.006	0.093	0.017	0.076	0.012	0.037	0.062	0.029	0.027
MgO	56.6	55.3	55.7	55.5	55.3	55.3	55.6	55.8	55.6	57.0	55.9	55.5
NiO	0.003	0.014	0.020	0.029	0.003	0.012	0.011	0.032	0.013	0.011	0.013	0.013
CaO	0.235	0.241	0.336	0.563	0.364	0.493	0.336	0.434	0.435	0.379	0.478	0.487
Sum	101.107	100.858	100.437	99.769	99.758	99.102	99.678	100.184	100.012	100.852	99.673	99.559

							Single grains				
Clast	7	8	8	9	C	C	E	1	2	2	5	6
Type	N	N	N	R	R	B	R	R	Bc	Rr	N	B
SiO_2	34.7	39.6	35.1	42.6	42.2	43.0	43.2	42.1	41.7	42.6	41.3	41.3
TiO_2	0.002	0	0.003	0.062	0.073	0.140	0.016	0	0.104	0.062	0.052	0.068
Al_2O_3	0.048	0.060	0.054	0.188	0.132	0.333	0.054	0.105	0.549	0.188	0.046	0.256
Cr_2O_3	0.589	0.258	0.409	0.486	0.185	0.144	0.348	0.328	0.075	0.486	0.615	0.156
FeO	46.3	16.3	26.3	0.494	0.475	0.382	0.968	0.601	0.313	0.494	10.2	0.637
MnO	0.442	0.200	0.310	0.332	0.054	0.028	0.450	0.043	0.003	0.332	0.366	0.009
MgO	19.3	43.3	34.9	55.6	56.3	56.8	57.0	56.4	55.4	55.6	47.7	56.1
NiO	0.099	0.040	0.059	0	0.009	0.003	0.034	0	0.006	0	0.013	0.024
CaO	0.112	0.098	0.122	0.454	0.227	0.433	0.056	0.126	0.803	0.454	0.264	0.360
Sum	101.592	99.856	97.257	100.216	99.665	101.263	102.126	99.703	98.953	100.216	100.556	98.910

Luminescence color: B blue, R red, N none. Core and rim of same grain shown by c and r. Clasts C and E are smaller than clasts 1–8.

Using a focused 25 kV beam with a sample current of ~100 namp on forsterite, peak and background data were obtained for Na, Mg, Al, Si, P, Ca, Ti, Cr, Mn, Fe and Ni. Calculated detection levels (2σ) based on the formula given in REED (1973) for minor elements are: Na_2O 50; Al_2O_3 85; P_2O_5 40; CaO 65; TiO_2 65; Cr_2O_3 75; MnO 80; NiO 150 ppm. For Na, P and Ni all measurements were near the detection level and the error is taken as the calculated detection level; for the other minor elements, errors based on counting statistics are approximately twice the detection limit. Because the count rates for Mg Kα (~30000 cps) and Si Kα (~10000 cps) were so high, they were used only for the matrix corrections; the values of MgO and SiO_2 in Table 1 are not of high accuracy. Chromium and Ti are given as Cr_2O_3 and TiO_2, but the possibility of divalent Cr and trivalent Ti should not be excluded (*cf.* SCHREIBER, 1977).

Cathodoluminescence photography was carried out using a propotype cathodoluminescence microscope and high-speed Ektachrome film with special processing. With a wide electron beam, there was a sharp distinction between three types of olivine; those with either blue or red or no luminescence. Unfortunately it is not possible to reproduce the photographs because of high printing cost, but they are available for inspection at The University of Chicago and are documented in STEELE (Geochim. Cosmochim. Acta, in press). The luminescence color was checked for each spot analyzed with the electron probe. Because the color changes as the diameter of the electron beam is changed, the color was determined with a broad beam before focusing to 5–10 μm beam for the minor-element analysis.

Points for analysis were selected from within the clasts described in the previous section as well as from single mineral clasts. Because most Mg-rich olivines luminesce, the variation in color was used as a guide for placing the beam on the grain and avoiding inclusions or polishing defects. Although most grains were chosen at random within any clast, special effort was made to include a range of luminescing colors and hence the analyses are weighted toward the rarer blue-luminescing grains. Twenty four representative analyses from the 80 obtained are given in Table 1.

4. Olivine Chemistry

In this section, we shall use the minor-element signature of olivine as a fingerprint for the B-7904 meteorite, and show how this signature is useful for classification of carbonaceous meteorites. Most previous workers have compared the carbonaceous meteorites mainly from textural observations and trace-element analyses (review: DODD, 1981). Olivine analyses were usually restricted to the Mg: Fe ratio with sparse data for Ca and Mn, the two easily detected minor elements. A notable exception is the study of Niger (I) by DESNOYERS (1980) who also analyzed Cr; however, the analytical precision is not as high as in the present study. For brevity, we shall compare the present data for olivines in B-7904 (Table 1; Fig. 4) with those for Murchison, another C2, and Allende, a CV3. Other data are given in STEELE *et al.* (1985a, b).

4.1. Minor elements in Belgica-7904 olivine

4.1.1. Iron

All the luminescent olivines have low FeO with concentrations ranging from 0.3

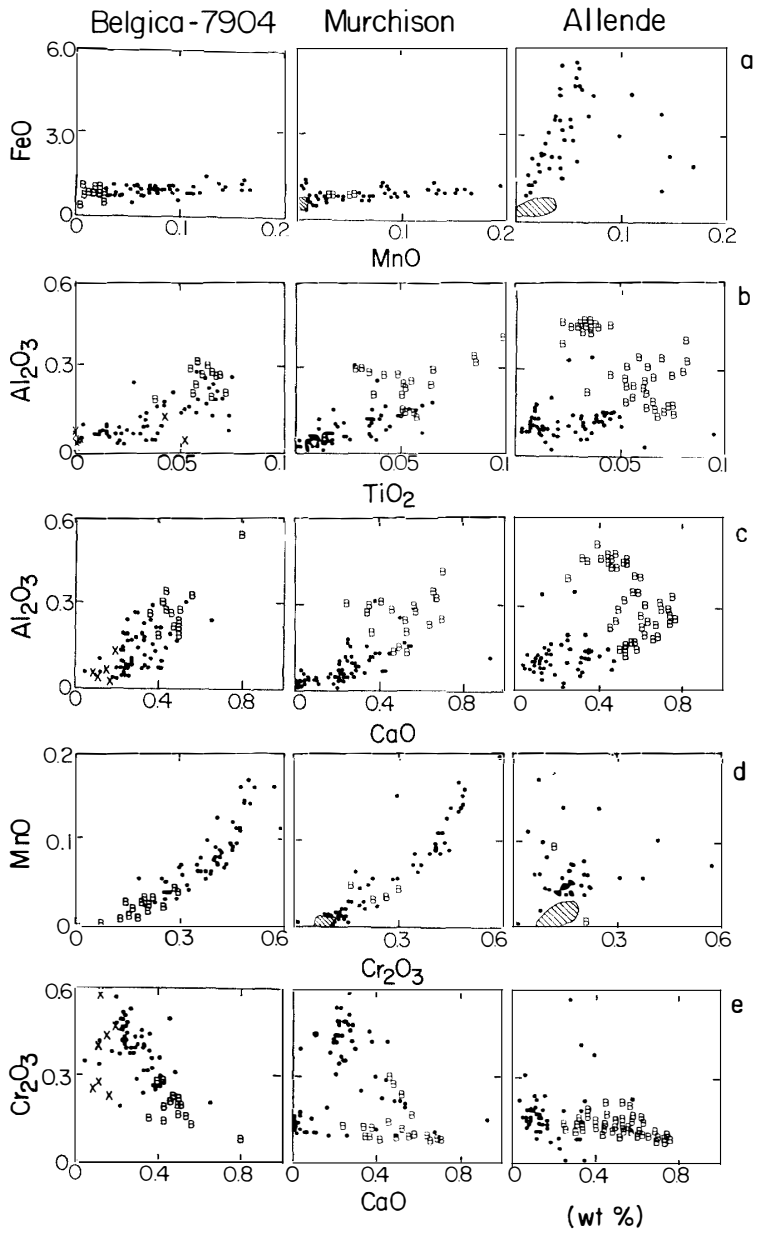

Fig. 4. Oxide plots for forsterites in B-7904, Murchison and Allende. Olivines with blue and red luminescence are distinguished by B and a dot respectively. Ruled areas denote high concentrations of B. Non-luminescent olivines in B-7904 are shown by a cross.

to 1.5 wt% FeO. The ranges overlap for the blue and red olivines (Fig. 4, upper left). The non-luminescent olivines from clasts #7 and #8 are much richer in FeO: clast #7, mainly Fo_{58-41}; clast #8, Fo_{83-67}. Because Mg-rich olivines occur in all carbonaceous meteorites (*e.g.* WOOD, 1967; MCSWEEN, 1977b), the presence of forsterite with an unspecified composition is not sufficient for classification of a carbonaceous meteorite into a subtype. However, the tight cluster of the olivine compositions at Fo_{98-99} in both B-7904, Murchison (FUCHS *et al.*, 1973) and other C2 meteorites appears characteristic, and distinguishes them from the Cl meteorites (*e.g.* ORGUEIL, to be published) and the CV3 meteorites (*e.g.* Allende with a continuous range from Fo_{99} to Fo_{90} and

beyond; upper right, Fig. 4). The Fe-rich non-luminescent olivines of B-7904 clasts #7 and #8 match with those in Type II chondrules (McSween, 1977a), in accordance with the textural resemblance.

4.1.2. Manganese

The level of Mn, and especially its correlation with Fe, has provided a useful criterion for recognition of different petrogenetic systems, especially among meteorite, lunar and terrestrial samples (*e.g.* achondrites; Smith *et al.*, 1983). In the Belgica forsterites (Fig. 4a), MnO varies from near the detection level to 0.17 wt%, and shows a positive correlation with Fe. The MnO-FeO variation for Murchison is almost identical, but the trend for Allende is quite different (Fig. 4a, right). Those forsterite grains which show blue luminescence clearly have the lowest Mn content (Fig. 4a). The non-luminescent olivines from B-7904 carry more Mn than the luminescent ones as expected because of the general correlation between Fe and Mn in all suites of olivine. However, the Fe/Mn ratio of these non-luminescent olivines increases strongly from about 30 for the Fe-poor ones to 80 for the Fe-rich ones in contrast to the relatively constant value for each type of achondritic olivine (Smith *et al.*, 1983).

4.1.3. Calcium

This element is relatively high in most of the forsterites in B-7904, and there is a wide range from 0.1 to 0.6 wt% CaO. The blue olivines tend to contain more Ca than the red ones. A simple comparison with terrestrial olivines from igneous rocks (Simkin and Smith, 1970) would suggest that the B-7904 olivines crystallized at a high temperature from a liquid, and were not annealed. Although this analogy would be inappropriate if the forsterites crystallized from a vapor, crystallization at high temperature is an obvious explanation of the high Ca content. The levels in the B-7904 forsterites are similar to those reported for forsterites from Vigarano, Murchison and Murray (Hutchison and Symes, 1972). McSween (1977b) noted a negative correlation of Ca with increasing FeO for his Type I chondrules in contrast to B-7904, but the near-constant FeO in the B-7904 forsterites rules out any significant correlation. The non-luminescent Fe-rich olivines from B-7904 contain 0.1 to 0.3 wt% CaO, which is still high, but not as high as for the forsterites.

4.1.4. Nickel

The low values of NiO in the luminescent forsterites are consistent with a reducing system, and fractionation of most of the Ni into a metal phase represented by the Ni-Fe inclusions. Among the forsterites from the carbonaceous chondrites, only those from the Orgueil Cl meteorite contain substantial NiO indicative of an oxidized state (Steele *et al.*, 1985a). Within experimental error, the Fe-rich olivines of B-7904 contain more NiO (130–990 ppm) than most of the forsterites (30–340 ppm). Because of the negative correlation between Fe and Ni in terrestrial olivines (Simkin and Smith, 1970), the possibility that the oxidation state was higher for the Fe-rich olivines than the forsterites in B-7904 should be explored.

4.1.5. Chromium

The forsterite olivines from the carbonaceous chondrites reach higher values of Cr_2O_3 (B-7904, 0.1–0.6 wt%, Fig. 4; Niger I (C2), 0.1–0.8 wt%, Desnoyers, 1980; Murchison, 0.1–0.6 wt%, Fig. 4; Bells (C2 or C1), 0.3–0.5 wt%, Davis and Olsen, 1984; Allende (CV3), mostly 0.1–0.2, but up to 0.6 wt%, Fig. 4; Orgueil (C1), 0.2–

0.5 wt%, STEELE *et al.*, 1985a) than any terrestrial olivines (DEER *et al.*, 1982, p. 47). Whether such high values of total Cr, expressed formally as Cr_2O_3, result from preferential partitioning of divalent Cr into olivine is not known. Although the presence of Ni-Fe inclusions in the C2 forsterites definitely testifies to a reduced state, and Cr is high in some lunar olivines (*e.g.* SCHREIBER, 1977), there is a strong temperature dependence for partitioning of both Cr^{2+} and Cr^{3+} between olivine and certain melt compositions (SCHREIBER, 1979). Even though the non-luminescent olivines of B-7904 are Fe-rich, they are also Cr-rich (0.26–0.61 wt%), and there is no tendency for Cr to be anticorrelated with Fe as in terrestrial olivines (SIMKIN and SMITH, 1970).

4.1.6. Aluminum

The large ranges of Al_2O_3 in the forsterite olivines from carbonaceous meteorites, and particularly the high values of the upper limits (B-7904, 0.35 wt%; Murchison, 0.4 wt%; Allende, 0.5 wt%; Orgueil, 0.3 wt%, STEELE *et al.*, 1985a) are remarkable. Most terrestrial and lunar olivines contain less than 0.05 wt% Al_2O_3, and the highest Al_2O_3 for a high-precision analysis is only 0.10 wt% in forsterites from high-temperature peridotite xenoliths in kimberlites (HERVIG, R. L. and SMITH, J. V., Earth Planet. Sci. Lett., submitted). [Higher values of Al_2O_3 in electron probe analyses of terrestrial and lunar olivines probably result from incorrect determination of the background near an absorption edge.] Aluminum-rich forsterite (Al_2O_3, 0.16–0.21 wt%) has been reported in complex spinel-olivine-forsterite inclusions in Allende (CLAYTON *et al.*, 1984) and in refractory inclusions in Murchison (MACPHERSON *et al.*, 1983) where the bulk composition is Al-rich. Other factors which may control the substitution of Al in olivine are temperature and rate of crystallization but the effect of each is unknown. The non-luminescent olivines consistently contain 0.05–0.06 wt% which is comparable to that in olivines from high-temperature lherzolites (HERVIG and SMITH, see above).

4.1.7. Titanium

Like Al_2O_3, TiO_2 is relatively high with a maximum of 0.1 wt% in the B-7904 forsterites. All high-precision analyses of TiO_2 in olivines from achondritic meteorites have less than 0.1 wt%, and forsterites from dunite xenoliths in kimberlites have a maximum of 0.05 wt% TiO_2 (DAWSON *et al.*, 1981). Again little is known about the factors controlling Ti substitution in olivine, and the above comments for Al are relevant. Titanium is low in the Fe-rich olivines from B-7904.

4.1.8. Sodium, phosphorous

Both elements are consistently near the detection level.

4.2. Interelement correlations and comparison with Murchison and Allende forsterites

The minor elements in B-7904 forsterites form two groups based on interelement correlations. The first group is composed of the refractory elements Ca, Al and Ti and each element shows a positive correlation with the other two as illustrated in Figs. 4b and 4c for Al *vs.* Ti and Al *vs.* Ca, respectively. Some of the scatter results from random experimental error, especially for the lower levels of Ti and Al. A second group of elements Fe, Cr and Mn also shows positive correlations (*e.g.* Fe *vs.* Mn, Fig. 4a; Mn *vs.* Cr, Fig. 4d). The two groups are negatively correlated (*e.g.* Cr_2O_3 *vs.* CaO, Fig. 4e). There is some overlap between the blue and the red forsterites,

except for MnO. These data are now compared with those for forsterites in Murchison (C2) and Allende (CV3).

All the plots of forsterites in B-7904 and Murchison are fairly similar as expected for their classification as C2. However, the Murchison plots contain an extra population of forsterite which is lacking in B-7904. This is seen most clearly in the plot of CaO *vs.* Cr_2O_3 (Fig. 4e). The red forsterites (dots) in Murchison fall into two clusters, only one of which matches with B-7904. The second cluster with $Cr_2O_3 < 0.18$ wt% and CaO < 0.2 wt% can also be detected on the CaO-Al_2O_3 plot, but is hard to find on the other plots without access to the original data. Tentatively we conclude that B-7904 lacks this second population of red forsterites which occurs as red rims on blue cores of some of the isolated grains, and that although Murchison and B-7904 are both C2 meteorites, a subtle difference can be recognized from minor element data for olivine.

When the C2 meteorites are compared to Allende (CV3) considerably greater differences can be seen (Fig. 4). For example: (a) the Fe *vs.* Mn data show a very different pattern and slope; (b) the Cr *vs.* Ca plot for red forsterites in Allende is similar to that for the unusual red forsterite in Murchison and does not include the grouping for red forsterites common to both C2 meteorites; (c) the Al *vs.* Ca plot for Allende shows a cluster at high Al_2O_3 (0.4–0.5) which comes from one large unusual grain.

The Fe-rich olivines in B-7904 are shown by crosses in Fig. 4, and we have not yet obtained comparative data for other carbonaceous chondrites.

5. Matrix Material

Analyses were made of the fine-grained material using an energy-dispersive system and a Reed-Ware procedure. Considerable variability was found even for a beam diameter of 15 μm. The first three analyses for the greenish-brown cryptocrystalline glass between forsterite crystals show similar compositions to the next three isotropic grains, but there are some minor differences which require further study. A notable feature of both sets is the lack of CaO, NiO and TiO_2, and the rather low values of

Table 2. Analyses of other components.

	1	2	3	4	5	6	7	8	9
SiO_2	44.1	44.5	32.1	39.0	40.5	32.5	31.1	21.9	21.9
Al_2O_3	4.5	5.9	6.4	4.8	4.7	3.9	3.3	2.6	3.0
Cr_2O_3	0.5	0.9	2.0	3.5	3.4	2.1	0	0	0
FeO	15.2	13.7	20.9	22.5	23.6	18.6	33.2	19.6	29.2
MgO	27.0	28.6	18.0	22.4	23.8	23.0	18.5	19.7	19.7
NiO	0	0	0	0	0	0	3.2	0.8	0.8
CaO	0	0	0	0	0	0	3.5	9.6	3.9
Na_2O	1.1	1.5	2.2	0.7	0	1.0	0.7	0	0.7
SO_3	0.6	0.5	1.4	1.4	1.5	1.6	1.3	6.0	16.5
Sum	93.0	95.6	83.0	94.3	97.5	82.7	94.8	80.2	95.7

1–3 Cryptocrystalline glass in clast #5. 4–6 Isotropic "grains" in clast #4. 7–9 General meteorite matrix.

Al_2O_3 (4–6 wt%). We conclude that the forsterites are not in equilibrium with the glasses and the isotropic grains. The general matrix of the B-7904 meteorite (last three analyses) shows considerable NiO (1–3 wt%), CaO (4–10 wt%), and SO_3 (1–16 wt%), and presumably consists of several phases including phyllosilicates (Table 2). Similar analyses were presented by FUCHS *et al.* (1973) for Murchison.

6. Discussion

Specifically for B-7904, the present data support its classification as a C2 meteorite. Although there is a general resemblance between the chemical and textural features of Murchison and B-7904, two properties are different: lack of Mg-pyroxene in B-7904, presence of a second type of red-luminescent forsterite in Murchison. We are now studying systematically all the C2 meteorites to determine whether these distinctions allow a subdivision into two types, or whether even further differences occur.

In general, the textural and chemical features reinforce the conclusion reached for Murchison and Allende that a simple scheme of forsterite growth from a vapor or a liquid is insufficient (STEELE *et al.*, 1985a). A detailed discussion will be prepared when further data are collected for various carbonaceous chondrites including Bells (DAVIS and OLSEN, 1984). Currently for B-7904, it seems necessary to propose at least the following stages in a complex scheme: (a) crystallization of blue-luminescent forsterite at high temperature from a reduced source rich in the refractory elements Al, Ti and Ca, (b) partial dissolution followed by enclosure of the blue olivine grains by either a red-luminescent forsterite or a non-luminescent Fe-rich olivine, (c) epitaxial growth of the red olivine on the blue olivine after the blue olivine became enclosed in a liquid, (d) alteration of some of the red olivine and all of the residual liquid to give cryptocrystalline glasses, (e) various processes of fragmentation and mechanical aggregation to produce a range of textures of the clasts containing red forsterites, including the fine-grained rims, (f) mechanical aggregation of two types of clasts into a fine-grained matrix which subsequently became hydroxylated.

Where these processes occurred, and whether the blue forsterites are relic grains that formed from a vapor, will be discussed elsewhere. In general, we note that B-7904 is yet another Antarctic meteorite which extends the range of properties of extraterrestrial materials and testifies to the marvelous range of processes in the early history of the solar nebula and interstellar space.

Acknowledgments

We thank Richard T. Cox for his early measurements of minor elements, N. WEBER and O. DRAUGHN for technical help, NASA for grant NAG 9–47, and particularly the National Institute of Polar Research for supplying B-7904.

References

BROWNLEE, D. E. (1981): Extraterrestrial components. The Sea, Vol. 7, ed. by C. EMILIANI. New York, Wiley, 733–762.

BROWNLEE, D. E., BATES, B. A. and WHEELOCK, M. M. (1984): Extraterrestrial platinum group nuggets in deep-sea sediments. Nature, **309**, 693–695.

BROWNLEE, D. E., TOMANDL, D. A. and OLSEWSKI, E. (1977): Interplanetary dust; A new source of extraterrestrial material for laboratory studies. Proc. Lunar Sci. Conf., 8th, 149–160.

CLAYTON, R. N., MACPHERSON, G. J., HUTCHEON, I. D., DAVIS, A. M., GROSSMAN, L., MAYEDA, T. K., MOLINE-VELSKO, C. and ALLEN, J. M. (1984): Two forsterite-bearing FUN inclusions in the Allende meteorite. Geochim. Cosmochim. Acta, **48**, 535–548.

DAVIS, A. M. and OLSEN, E. (1984): Bells—A carbonaceous chondrite related to C1 and C2 chondrites. Lunar and Planetary Science XV. Houston, Lunar Planet. Inst., 190–191.

DAWSON, J. B., HERVIG, R. L. and SMITH, J. V. (1981): Fertile iron-rich dunite xenoliths from the Bultfontein kimberlite, South Africa. Fortschr. Mineral., **59**, 303–324.

DEER, W. A., HOWIE, R. A. and ZUSSMAN, J. (1982): Rock-Forming Minerals. Vol. 1A. Ortho- and silicates. London, Longman.

DESNOYERS, C. (1980): The Niger (I) carbonaceous chondrite and implications for the origin of aggregates and isolated olivine grains in C2 chondrites. Earth Planet. Sci. Lett., **47**, 223–234.

DODD, R. T. (1981): Meteorites; A Petrologic-Chemical Synthesis. Cambridge, Cambridge Univ. Press, 368 p.

FUCHS, L. H., OLSEN, E. and JENSEN, K. J. (1973): Mineralogy, mineral-chemistry, and composition of the Murchison (C2) meteorite. Smithson. Contrib. Earth Sci., **10**, 39 p.

HUTCHISON, R. and SYMES, R. F. (1972): Calcium variation in olivines of the Murchison and Vigarano meteorites. Meteoritics, **7**, 23–29.

MACPHERSON, G. J., BAR-MATTHEWS, M., TANAKA, T., OLSEN, E. and GROSSMAN, L. (1983): Refractory inclusions in the Murchison meteorite. Geochim. Cosmochim. Acta, **47**, 823–839.

MCSWEEN, H. Y., Jr. (1977a): Chemical and petrographic constraints on the origin of chondrules and inclusions in carbonaceous chondrites. Geochim. Cosmochim. Acta, **41**, 1843–1860.

MCSWEEN, H. Y., Jr. (1977b): On the nature and origin of isolated olivine grains in carbonaceous chondrites. Geochim. Cosmochim. Acta, **41**, 411–418.

NATIONAL INSTITUTE OF POLAR RESEARCH (1982): Belgica-7904. Meteorites News, **1**, 26.

OLSEN, E. and GROSSMAN, L. (1978): On the origin of isolated olivine grains in type 2 carbonaceous chondrites. Earth Planet. Sci. Lett., **41**, 111–127.

RAMBALDI, E. R. (1981): Relict grains in chondrules. Nature, **293**, 558–561.

RAMBALDI, E. R., RAJAN, R. S., WANG, D. and HOUSLEY, R. M. (1983): Evidence for relict grains in chondrules of Qingzhen, an E3 type enstatite chondrite. Earth Planet. Sci. Lett., **66**, 11–24.

REED, S. J. B. (1973): Principles of X-ray generation and quantitative analysis with the electron microprobe. Microprobe Analysis, ed. by C. A. ANDERSEN. New York, Wiley, 53–81.

RICHARDSON, S. M. and MCSWEEN, H. Y., Jr. (1978): Textural evidence bearing on the origin of isolated olivine crystals in C2 carbonaceous chondrites. Earth Planet. Sci. Lett., **37**, 485–491.

SCHREIBER, H. D. (1977): Redox states of Ti, Zr, Hf, Cr, and Eu in basaltic magmas; An experimental study. Proc. Lunar Sci. Conf., 8th, 1785–1807.

SCHREIBER, H. D. (1979): Experimental studies of nickel and chromium partitioning into olivine from synthetic basaltic melts. Proc. Lunar Planet. Sci. Conf., 10th, 509–516.

SIMKIN, T. and SMITH, J. V. (1970): Minor-element distribution in olivine. J. Geol., **78**, 304–325.

SMITH, J. V., STEELE, I. M. and LEITCH, C. A. (1983): Mineral chemistry of the shergottites, nakhlites, Chassigny, Brachina, pallasites and ureilites. Proc. Lunar Planet. Sci. Conf., 14th, Pt. 1, B229–B236 (J. Geophys. Res., **88** Suppl.).

STEELE, I. M., COX, R. T., Jr. and SMITH, J. V. (1984): Belgica 7904, an extreme C2 from Antarctica; Petrology and mineral chemistry (abstract). Lunar and Planetary Science XV. Houston, Lunar Planet. Inst., 820–821.

STEELE, I. M., SMITH, J. V. and SKIRIUS, C. (1985a): Cathodoluminescence zoning and minor elements in forsterites from the Murchison (C2) and Allende (C3V) carbonaceous chondrites. Nature, **313**, 294–297.

STEELE, I. M., SMITH, J. V. and BROWNLEE, D. E. (1985b): Minor-element signature of relic olivine grains in deep-sea particles; A match with forsterite from C2 meteorites. Nature, **313**, 297–299.

WOOD, J. A. (1967): Olivine and pyroxene compositions in Type II carbonaceous chondrites. Geochim. Cosmochim. Acta, **31**, 2095–2108.

(*Received November 12, 1984; Revised manuscript received October 1, 1985*)

Appendix. Descriptions of 9 Clasts in Belgica-7904

Clast #1

One mm diameter subround, zoned olivine-glass clast. Center composed of fine-grained (<5 μm) sulfide and silicate. Middle-zone contains coarse subhedral olivine up to 0.2 mm. Many grains are in optical continuity with adjacent grains. Intergranular sulfide is rare and interstices contain dark brown cryptocrystalline glass. Olivine grains contain rare blebs of metal and common round inclusions of greenish-brown glass(?). Nearly all olivine grains show good extinction but most grains show trails of defects and inclusions. The outer zone is composed of fine, equigranular olivine of ~ 20 μm size with an equal area of brown cryptocrystalline glass. The boundary between the coarse olivine zone and the outer zone is sharp while the boundary of the outer zone with the matrix, although sometimes sharp, often interfingers with matrix. Where a sharp outer zone-matrix boundary is present, the adjacent matrix is opaque but where a poorly defined boundary is present the adjacent matrix is similar to the general meteorite matrix. All olivine grains show red luminescence.

Clast #2

Amoeboid-shaped inclusion, 1.1 mm in longest dimension composed of loosely aggregated 5–35 μm anhedral olivine grains and abundant greenish-brown glass. Olivine: glass=20: 80. Some olivine grains are quite irregular in shape having prominent recesses and occasional angular edges. Nearly all contain several very small 1–8 μm round brown glass (?) inclusions. In addition to the olivine, there are other grains ($\sim 15\%$ of clast) with similar sizes and shapes but which are composed of the greenish-brown glass. These grains are visible with transmitted light due to darker borders but are isotropic. Most occur near margin of the clast. A 50–500 μm black fine-grained matrix shell surrounds the inclusion and sharply terminates against its irregular boundary. The outer edge of the matrix shell is less well-defined and in places seems to grade into the general matrix. A few small olivine grains and portions of the large inclusion are contained within the matrix shell, and it is not clear from a 2D slice whether they are part of the inclusion or separated from it. All olivine grains show red luminescence.

Clast #3

Subround, 0.5 mm granular aggregate of ~ 20 μm anhedral olivine in the center and greenish-brown cryptocrystalline glass in an outer zone. The outer zone thickness is variable from 100 μm to near absent and gives a more evenly rounded appearance to the clast. Contained within the outer zone are a few isotropic grains like those described for clast #2. The outer zone is surrounded by a dark matrix zone or shell

that is ~50 μm wide and has a sharp boundary with the glass. Tiny inclusions of metal and silicate glass are present in the olivines but sulfide is absent. All olivine grains show red luminescence.

Clast #4

Because of their close proximity, these two inclusions might be considered halves of the some clast. The polygranular aggregates are each about 0.5 mm in diameter and are composed of anhedral to subhedral ~30 μm olivine grains and greenish-brown glass. One shows an irregular band of coarsely crystalline olivine. The glassy grains described for clasts #2 and #3 are present and comprise about 5–10% of both inclusions. Tiny round 1–10 μm inclusions occur in most grains although some are colorless instead of the usual brown. Very minor amounts of sulfides are present as inclusions within some olivine grains. Clast boundaries are distinct and a dark matrix shell varying in thickness from 20–200 μm is present around both halves. Olivine: glass=65: 35. Tiny crystalline fragments in the general matrix tend to be aligned around portions of the outer shell. All small olivines show red luminescence, and olivines in the irregular band show blue luminescence; some blue olivines at the edge of the band have incomplete rims of red olivine.

Clast #5

Irregular 0.50×0.75 mm aggregate of anhedral to subhedral olivine grains averaging 20 μm. Brown cryptocrystalline glass composes ~25% of the inclusion in irregular patches. Numerous round brown glass inclusions are contained within the olivine grains; metal inclusions in olivine are rare. Many olivine grains show incomplete or undulose extinction. The matrix-clast boundary is sharp and the opaque matrix shell is 50 μm wide. All olivines show red luminescence.

Clast #6

Subround ~0.6 mm aggregate composed of olivine grains from 20 to 200 μm and greenish-brown cryptocrystalline glass. Olivine: glass=60: 40. The olivine grains are anhedral to subhedral and some have embayments filled with glass. Most contain 2–25 μm round brown glass inclusions. A few of the olivine grains show incomplete or undulose extinction similar to clast #5. A 25–100 μm matrix shell completely surrounds the clast and the matrix-clast boundary is sharp. A few brown grains similar to those described for clasts #2, #3 and #4 are present. All olivines show red luminescence.

Clast #7

Cluster of several subhedral olivine grains. The largest (300×350 μm) at the upper left is nearly continuous optically; some fragments of this grain are slightly rotated from the overall optical orientation. A smaller 150×175 μm crystal (just below center) shows well-developed morphology. An aggregate of three olivine grains (right of center) appears to be attached to the rest of the clast by greenish-brown glass partially surrounding the larger crystals. Grain–glass boundaries are primarily straight. Glass also occurs within olivine grains as small rounded and large stringer-like inclusions along the prominent fractures. Two opaque phases are present and occur only in the green-brown glass as large (50–120 μm) patches or as

finely disseminated grains. Olivine: glass: opaques=60: 30: 10. A dark matrix shell is absent. The large grains are Fe-rich and lack luminescence. The inner part of a small olivine grain in the attached aggregate shows blue luminescence, and the outer part lacks luminescence.

Clasts #8 and #9

Clast #8 is mainly composed of a 400 μm single olivine grain showing some crystal faces. Remainder of clast is terminated by edge of section and is composed of greenish-brown glass and blocky, angular olivine. The boundaries of the large olivine are slightly embayed and have small patches of glass attached. A dark matrix shell is absent and the general meteorite matrix is in contact with this clast. All olivines lack luminescence and are iron-rich. Clast #9 at the left contains small, irregular olivines set in greenish-brown glass. All olivines show red luminescence.